Near-wall turbulence modeling for boundary layers with separation

By S. H. Ko

1. Motivation and objectives

As a turbulent boundary layer undergoes a strong adverse pressure gradient, the flow may separate from the wall, and the use of empirical wall functions is inappropriate. The turbulence transport equations as well as the momentum equations must be solved through the laminar sublayer to the wall. The laminar sublayer encompasses a region where viscous effects become increasingly important. For the past two decades, many proposals for near-wall turbulence models of k-ϵ type have been presented for calculating near-wall flows. A thorough review and a systematic evaluation of these models was given by Patel, Rodi, and Scheuerer (1985): they found that some of the models tested failed to reproduce even the simple flat-plate boundary layer flow. Overall, the authors concluded that the near-wall turbulence models needed further refinement if they were to be used with confidence to calculate near-wall flows.

Recently, the use of a direct numerical simulation (DNS) data base has provided new insight and data for development and testing of near-wall turbulence models. Mansour, Kim, and Moin (1989) computed the budgets for the turbulence kinetic energy and its dissipation rate using DNS data of a channel flow (Kim, Moin, and Moser, 1987). These computed budgets were used to test existing near-wall turbulence models. They also analyzed the dependence of the eddy-viscosity damping function f_μ on y^+ and the Reynolds number using DNS data for a flat-plate boundary layer (Spalart, 1988). Durbin (1991) proposed the k-ϵ-v model. By using normal fluctuation $\overline{v^2}$ as a velocity scale instead of turbulence kinetic energy k in the eddy-viscosity relation, the k-ϵ-v model eliminated the need for damping functions f_μ . The model retained a modeled equation for $\overline{v^2}$ in addition to the k and ϵ equations. This model was implemented into a parabolic program and showed satisfactory agreement with the DNS data of the channel and boundary layer flows (see article by Durbin in this volume).

The objectives of the present study are : (a) to implement the k-ϵ-v model into a computer program which embodies the complete elliptic form of the 2-D, incompressible Navier Stokes equations for steady-state turbulent flows, (b) to make an assessment of the k-ϵ-v model by comparing predictions with DNS data as well as experimental measurements for various turbulent flows, (c) to make improvements and extensions of the modeling, if warranted, and (d) to provide the application of the k-ϵ-v model for predicting separated boundary layer flows. At the present state of the research, the implementation has been completed and the assessment is in progress. In this report, a brief summary of numerical methods is presented, followed by results of testing of the numerical methods. The implementation of the

k-ϵ-v has been confirmed by comparing predictions with the DNS data of the channel flow at $Re_\tau = 180$. In order to assess the new model, a series of computations will be compared with measurements of popular test cases covering several types of turbulent flow.

2. Accomplishments

The accuracy of a numerical prediction rests on the excellence of the turbulence model as well as on the accuracy of the numerical methods used to solved the modeled equations. For simple turbulent flows, most of the difficulties associated with numerical predictions are the lack of physical understanding and consequent inadequacies in the various turbulence models used. On the other hand, for complex turbulent flows, not only the turbulence models but also the numerical methods are in question. As the first step of the study, the accuracy of the numerical methods was investigated.

2.1 Numerical methods

2.1.1 Governing equations

The governing equations for conservation of mass, momentum, and transport of k, ϵ, $\overline{v^2}$, and $\mathcal{P}_{22}$ are :

$$\frac{\partial U_i}{\partial x_i} = 0. \tag{1}$$

$$\frac{\partial U_i}{\partial t} + \frac{\partial}{\partial x_j} U_i U_j = -\frac{1}{\rho}\frac{\partial P}{\partial x_i} + \frac{\partial}{\partial x_j}\left\{(\nu + \nu_t)\left(\frac{\partial U_i}{\partial x_j} + \frac{\partial U_j}{\partial x_i}\right)\right\} \tag{2}$$

$$\frac{\partial k}{\partial t} + U_k \frac{\partial k}{\partial x_k} = \mathcal{P} - \epsilon + \frac{\partial}{\partial x_k}\left(\nu \frac{\partial k}{\partial x_k} + \frac{\nu_t}{\sigma_k}\frac{\partial k}{\partial x_k}\right) \tag{3}$$

$$\frac{\partial \epsilon}{\partial t} + U_k \frac{\partial \epsilon}{\partial x_k} = C_{\epsilon 1}\frac{\mathcal{P}}{T} - C_{\epsilon 2}\frac{\epsilon}{T} + \frac{\partial}{\partial x_k}\left(\nu \frac{\partial \epsilon}{\partial x_k} + \frac{\nu_t}{\sigma_\epsilon}\frac{\partial \epsilon}{\partial x_k}\right) \tag{4}$$

$$\frac{\partial \overline{v^2}}{\partial t} + U_k \frac{\partial \overline{v^2}}{\partial x_k} = \mathcal{P}_{22} - \frac{\overline{v^2}}{T} + \frac{\partial}{\partial x_k}\left(\nu \frac{\partial \overline{v^2}}{\partial x_k} + \frac{\nu_t}{\sigma_k}\frac{\partial \overline{v^2}}{\partial x_k}\right) \tag{5}$$

$$L^2 \nabla^2 f_{22} - f_{22} = \frac{(1 - C_2)}{T}\left(\frac{2}{3} - \frac{\overline{v^2}}{k}\right) - C_1 \frac{\mathcal{P}}{k} \tag{6}$$

where ν_t is the eddy viscosity

$$\nu_t = C_\mu \overline{v^2} T, \tag{7}$$

T is the time-scale for the evolution of ϵ

$$T = max(k/\epsilon, C_T(\nu/\epsilon)^{1/2}), \tag{8}$$

$\mathcal{P}$ is the production of turbulence kinetic energy

$$\mathcal{P} = -\overline{u_i u_j}\frac{\partial U_i}{\partial x_j}, \tag{9}$$

$\mathcal{P}_{22}$ is a source term which combines the effects of pressure-velocity correlation and anisotropic dissipation

$$\mathcal{P}_{22} = k f_{22}, \tag{10}$$

and the length scale L is expressed as

$$L = C_L \, max(k^{3/2}/\epsilon, C_\eta(\nu^3/\epsilon)^{\frac{1}{4}}). \tag{11}$$

Detailed discussion of the k-ϵ-v model and its boundary conditions can be found in the report by Durbin (1991).

2.1.2 Numerical procedure

The k-ϵ-v model was implemented into a finite difference computer code developed for solving the 2-D, incompressible, steady-state turbulent flows. This program is based on previous finite difference procedures used in the TEACH computer program of Gosman and Pun (1974).

The governing equations (1) through (5) may be expressed in the general form

$$\frac{\partial}{\partial x}(U\phi) + \frac{\partial}{\partial y}(V\phi) - \frac{\partial}{\partial x}(\nu_e\frac{\partial \phi}{\partial x}) - \frac{\partial}{\partial y}(\nu_e\frac{\partial \phi}{\partial y}) = S_\phi \tag{12}$$

where ϕ represents any of the dependent variables, ν_e is the effective viscosity, and the source S_ϕ contains any remaining terms. The primitive variables are solved on a system of staggered grids. This discretization is based in all cases on the control volume approach which ensures that the conservation principle embodied in the continuum equations is preserved in the numerical analog. Following this approach, the governing equations are formally integrated over the appropriate control volume by applying the Gauss theorem.

The result is

$$\left\{U\phi - \nu_e\frac{\partial \phi}{\partial x}\right\}_e A_e - \left\{U\phi - \nu_e\frac{\partial \phi}{\partial x}\right\}_w A_w$$

$$+\left\{V\phi - \nu_e\frac{\partial \phi}{\partial y}\right\}_n A_n - \left\{V\phi - \nu_e\frac{\partial \phi}{\partial y}\right\}_s A_s = S_\phi V_c \tag{13}$$

where the A's represent the areas of the cell faces in four compass-point directions (n,e,s,w) located mid-way between the grid points, and V_c represents the volume of the cell.

The next step in formulating a finite differencing equation is the assumption of the ϕ profiles between any two grid points. The diffusion terms are formulated using a central differencing scheme; since this is common practice, nothing further need be said about them. Attention is directed to the convection terms, for it is the approximations that are used for these terms that can lead to the generation of

artificial viscosity. The schemes that are used to approximate the convective terms only refer to the differencing of convected quantity ϕ; the convecting velocity is discretized using the central differencing scheme. In the present computer code, the QUICK (Quadratic Upstream-weighted Interpolation for Convection Kinematics) differencing scheme of Leonard (1979) was used in order to reduce the error due to the artificial viscosity.

Upon collecting terms in the finite difference equations, the generic differential equation can be put into the discretized form

$$B_P^\phi \phi_P = \sum_j B_j^\phi \phi_j + S_u \tag{14}$$

where

$$B_P^\phi = \sum_j B_j^\phi - S_P. \tag{15}$$

Here the subscript j denotes the neighbor grid points of the point P. The B's are coefficients consisting of contributions from diffusion and convection, and the S's are the linearized source terms. Obviously, the B's and S's are uniquely formulated for each differencing scheme.

The direct methods for solving the above finite difference equations require excessive storage and computer time. Therefore, an iterative method for solving the algebraic equations is employed. The computation sequence starts with guesses for the velocity field and related quantities. For the first step, the SIMPLER (Semi-Implicit Method for Pressure Linked Equations, Revised) algorithm of Patankar (1980) is used for obtaining the pressure field from the pressure equation which is derived from the continuity and momentum equations. Next, the axial and radial momentum equations are solved for U and V velocity components, respectively. Then, in order to conserve mass locally, a correction of velocity is completed via a with the pressure-correction equation, which is also derived from the continuity and momentum equations. Finally, the turbulence transport equations are solved, and the effective viscosity is updated accordingly. The newly obtained flowfield is treated as an improved guess and the process returns to the first step. This iterative procedure continues until convergence.

The discretization equations are linear and are solved line-by-line using the Tri-Diagonal-Matrix Algorithm (TDMA) applied in an ADI (Alternating Direction Implicit) manner.

2.2 Testing of numerical techniques

2.2.1 Laminar flow in a driven cavity

A driven cavity problem has been an ideal non-linear problem for testing new numerical schemes and as a benchmark solution for making comparisons among various schemes using different methods of problem formulation, discretization, iteration, and approximation. The geometry and the boundary conditions for the flow are the same as those of the Kim & Moin's (1985) computation.

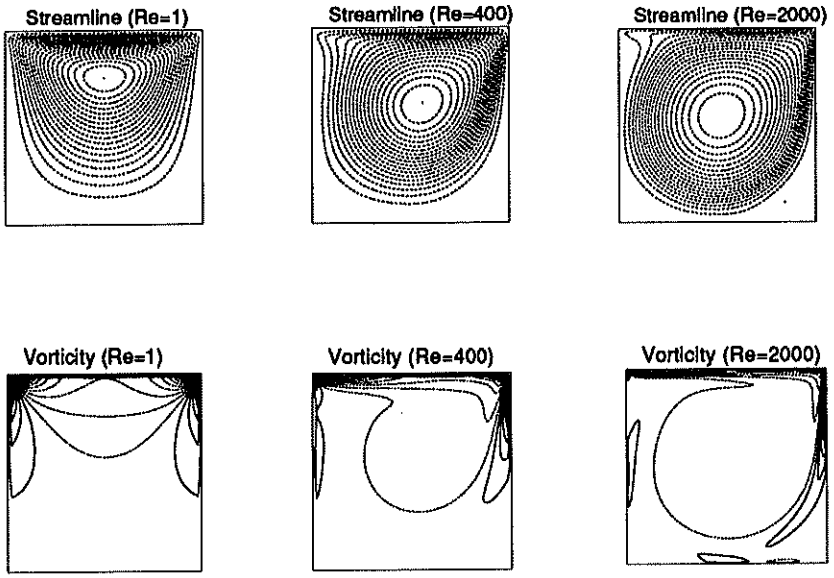

FIGURE 1. Streamlines and contours of constant vorticity for a driven cavity

After grid independence testing, final predictions were made with two different uniform grids: a 50×50 grid for flows with $Re < 1000$ and a 100×100 grid for flows with $Re \geq 1000$. Three differencing schemes (QUICK, central, hybrid) were tested for this problem with Reynolds numbers up to 5000. However, a converged solution could not be obtained for $Re = 5000$ with the central differencing scheme.

Predictions are compared with those by Kim & Moin (1985) and by Ghia *et al.*(1982). Figure 1 shows the predicted streamlines and contours of constant vorticity for three different Reynolds numbers. At $Re = 1$, the streamlines are symmetric because the convection terms are negligible. At $Re = 400$, these convection terms have begun to dominate the flow, producing a core of nearly uniform vorticity. Note that the vortex center shifts in the direction of the boundary velocity. At $Re = 2000$, the core of the primary vortex becomes almost inviscid and shows a symmetric structure about the center of the circle. As observed by Kim & Moin, a secondary vortex starts to develop at the upper-left corner of the cavity at this Reynolds number.

Figure 2 shows the distribution of the streamwise velocity at the middle plane of the cavity for $Re = 400$. The present solution shows close agreement with the solution by Kim and Moin (1985). Since the non-linear effect of the convection is small, the QUICK, the central, and the hybrid schemes show little difference. However, as shown in Fig. 3, these schemes show a significant difference when the Reynolds number is high. It is obvious that the hybrid scheme suffers from artificial viscosity. Overall, it is found that the QUICK scheme is stable and accurate, the central differencing scheme is accurate but unstable, and the hybrid differencing scheme is stable but inaccurate. Figures 4 and 5 show the predicted stream-function and vorticity at the center of the primary vortex, respectively. As observed previously,

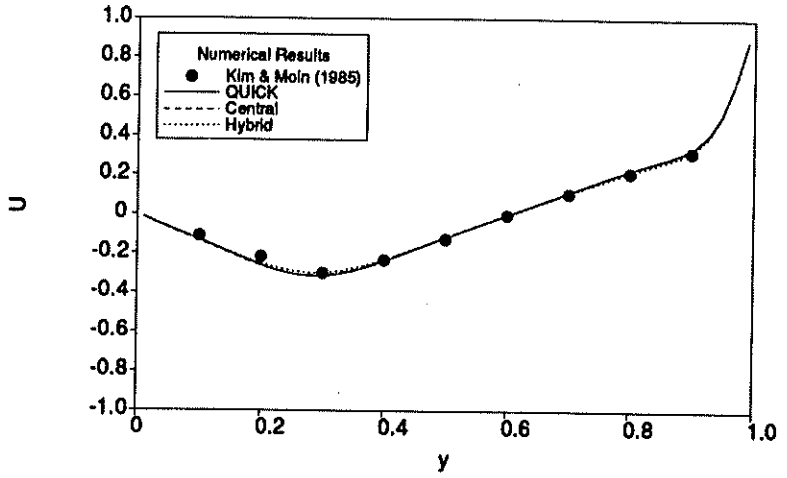

FIGURE 2. Streamwise velocity at the midplane of the cavity for $Re = 400$

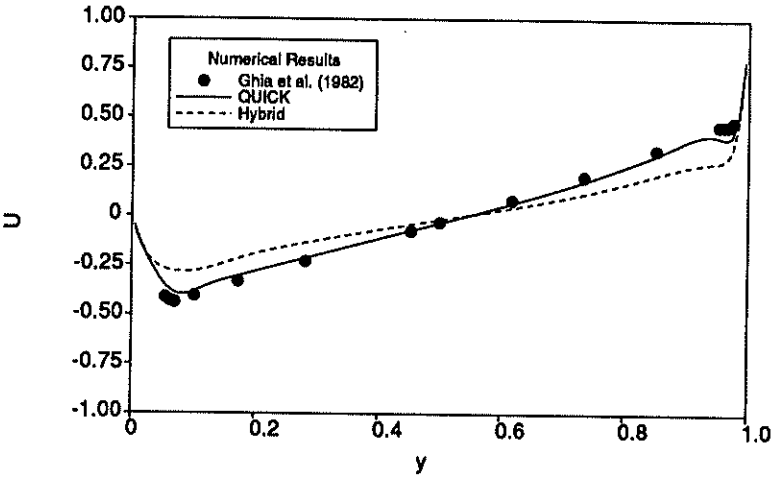

FIGURE 3. Streamwise velocity at the midplane of the cavity for $Re = 5000$

the QUICK scheme provides the most reliable solutions.

2.2.2 Laminar flow over a backward-facing step

For the second test problem, the laminar flow over a backward-facing step has been chosen. The detailed description of the problem can be found in the work of Kim and Moin (1985). A 100 × 100 uniformly-spaced grid was used for the computations.

Figure 6 shows predicted reattachment lengths in comparison with the experimental and the computational results of Armaly *et al.* (1983) and the numerical results

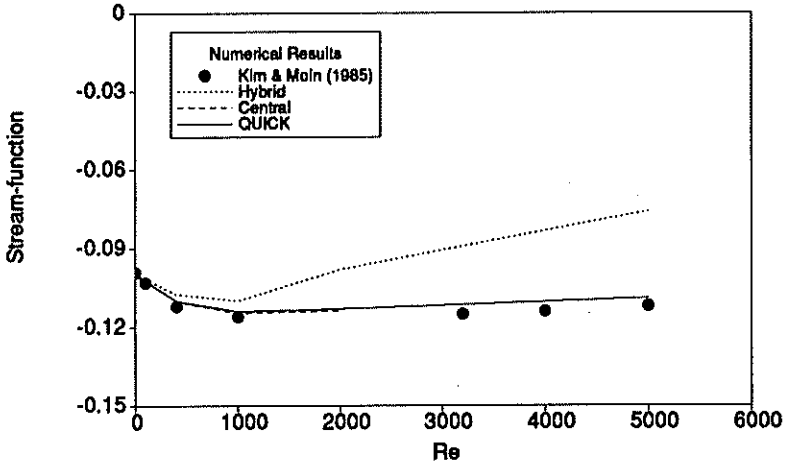

FIGURE 4. Stream-function at the center of the primary vortices for different Reynolds numbers

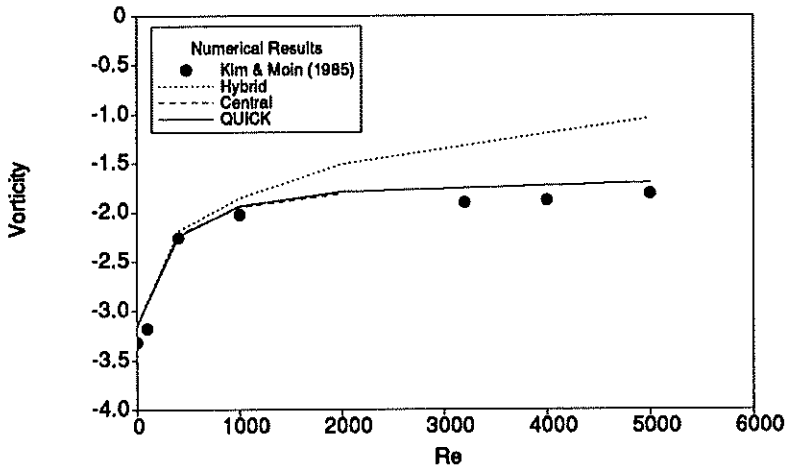

FIGURE 5. Vorticity at the center of the primary vortices for different Reynolds numbers

of Kim and Moin (1985). Using the central differencing scheme, converged solutions were obtained for flows with Reynolds numbers up to 600. It should be noted that Armaly *et al.* (1983) used an upwind differencing scheme for the convective terms. That might explain why his computations show such a poor performance. The QUICK scheme shows its ability in predicting the reattachment length fairly well.

The length of the secondary bubble on the flat upper wall is a good indication for the performance of the numerical schemes. Figure 7 shows a comparison of the

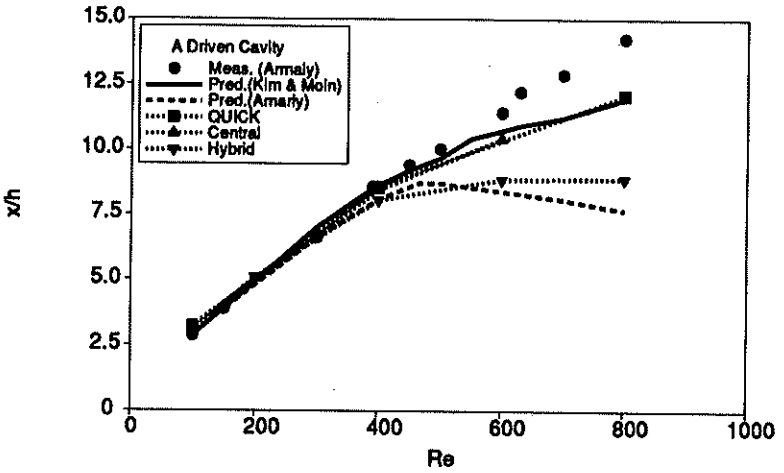

FIGURE 6. Reattachment length as a function of Reynolds number

bubble lengths predicted by two different numerical methods: the present TEACH type program and the Kim & Moin's program. The predicted bubble lengths by the present program, using the QUICK scheme, show excellent agreement with those by Kim & Moin's program.

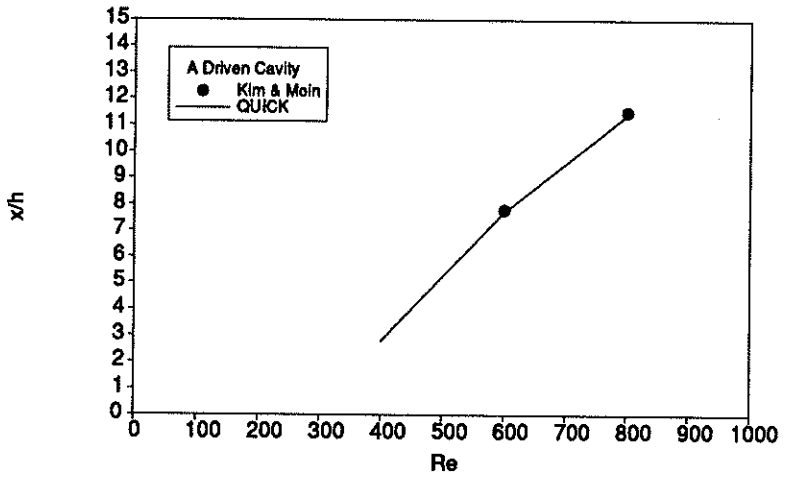

FIGURE 7. Secondary bubble length as a function of Reynolds number

2.3 Testing of the k-ε-v model

The k-ϵ-v model was implemented into the program described in Sec. 2.1.2. In order to confirm the correct implementation of the k-ϵ-v model, the channel flow at $Re_\tau = 180$ was selected as the first test case. As expected, the predicted profiles

of the streamwise velocity and the turbulence quantities were almost identical to those reported by Durbin (1991).

Testing of the present implementation of the k-ϵ-v model is continuing. The zero pressure gradient boundary layer is being computed and compared with measurements by Wieghardt and Tillmann (1951). This boundary layer is the simplest case of wall turbulent flows, yet it is of great practical importance. It provides a starting point for the computation of separated boundary layers.

Separated boundary layers are quite different from zero pressure gradient boundary layers in many ways: (a) they are elliptic, *i.e.* the pressure distribution upstream of separation is influenced by the flow downstream of separation, (b) the Prandtl's boundary layer assumptions are no longer valid due to the rapid increase of the boundary layer thickness, and (c) the curvature of the streamlines near the separation has a strong influence on the degree of anisotropy between the normal Reynolds stresses (Bradshaw, 1973). All these facts make the separated boundary layers hard to predict correctly.

3. Future plans

The main objective of the research is to develop a near-wall turbulence model which simulates a large variety of types of flow without ad hoc adjustment. Also, the model has to be easy to use. Therefore, the main difficulties of the model development is to select a universal set of differential equations and then to provide the required closure constants. In this point of view, the equations of the k-ϵ-v model, originally developed by Durbin (1991), will be carefully extended and improved for two dimensional elliptic problems.

In order to account for the anisotropy of the turbulence stresses, the possibility of using the tensorial form of the eddy viscosity will be studied, *i.e.*

$$\nu_{ij} = C_\mu \overline{u_i u_j} T. \tag{16}$$

Furthermore, the effects of streamline curvature will be incorporated in the modeling. This incorporation can be achieved either by modifying the ϵ equation (Launder *et al.*, 1977) or by modifying the expression of the eddy viscosity ν_t (Bradshaw, 1973). These new features of the modeling will, of course, make the modeling more complicated, which is not always desirable.

To evaluate the practical application of the improved k-ϵ-v model, a study of the momentum and thermal details of separated boundary layers with heat transfer will be undertaken. As the first attempt, a specified normal velocity distribution along the free stream boundary will be given in an effort to match a selected experimental pressure distribution along the wall. This matching may require an iterative procedure. Solutions by the improved k-ϵ-v model will be compared with solutions by DNS (Moin, 1991) which is in progress. Prescribed wall temperature distribution and/or wall heat flux distribution will be added later.

REFERENCES

ARMALY, B. F., DURST, F., PEREIRA, J. C. F., & SCHÖNUNG, B. 1983 Experimental and theoretical investigation of backward-facing step flow. *J. Fluid*

Mech. **127**, 473-496.

BRADSHAW, P. 1973 Effects of streamline curvature on turbulent flows. AGARDograph. No. 169.

DURBIN, P. A. 1991 Near-wall turbulence closure modeling without "damping functions". *Theoretical and Computational Fluid Dynamics.* **3**, 1-13.

GHIA, U., GHIA, K. N. & SHIN, C. T. 1982 High-Re solutions for incompressible flow using the Navier-Stokes equations and a multigrid method. *J. Comput. Phys.* **48**, 387-411.

GOSMAN, A. D. & PUN, W. M. 1974 Calculation of recirculating flows. Research Report No. HTS/74/2. Dept. Mech. Engr. Imperial College. London, England.

KIM, J. & MOIN, P. 1985 Application of a fractional-step method to incompressible Navier-Stokes equations. *J. Comput. Phys.* **59**, 308-323.

KIM, J, MOIN, P., & MOSER, R. 1987 Turbulence statistics in fully developed channel flow at low Reynolds number. *J. Fluid Mech.* **177**, 133-166.

LAUNDER, B. E., PRIDDIN, C. H., & SHARMA, B. I. 1977 The calculation of turbulent boundary layers on spinning and curved surfaces. *J. Fluids Engr.* 231-239.

LEONARD, B. P. 1979 A stable and accurate convective modeling procedure based on quadratic upstream interpolation. *Computer Methods in Applied Mechanics and Engineering.* **19**, 59-98.

MANSOUR, N. N., KIM, J. & MOIN, P. 1989 Near-Wall k-ϵ Turbulence Modeling. *AIAA J.* **27**, 1068-1073.

MOIN, P. 1991 Private communication.

PATANKAR, S. V. 1980 *Numerical heat transfer and fluid flow.* McGraw-Hill. New York.

PATEL, V. C., RODI, W., & SCHEUERER, G. 1985 Turbulence models for near-wall and low Reynolds number flows : A review. *AIAA J.* **23**, 1308-1319.

SPALART, P. R. 1988 Direct simulation of a turbulent boundary layer up to Re_θ = 1400. *J. Fluid Mech.* **187**, 61-98.

WIEGHARDT, K. & TILLMAN, W. 1951 On the turbulent friction layer for rising pressure. NACA TM 1314.